Title
Heterogeneous expression of multiple putative patterning genes by single cells from the chick hindbrain.

Journal
Developmental biology, 191(2)

ISSN
0012-1606

Authors
Kato, Keiko
O'Dowd, Diane K
Fraser, Scott E
et al.

Publication Date
1997-11-15

DEVELOPMENTAL BIOLOGY **191,** 259–269 (1997)
ARTICLE NO. DB978717

Heterogeneous Expression of Multiple Putative Patterning Genes by Single Cells from the Chick Hindbrain

Keiko Kato,*,[1] Diane K. O'Dowd,† Scott E. Fraser,* and Martin A. Smith†

**Division of Biology, California Institute of Technology, Pasadena, California 91125; and*
†*Department of Development and Cell Biology and Department of Anatomy and Neurobiology, University of California at Irvine, Irvine, California 92697-1280*

The metameric organization of the vertebrate hindbrain into rhombomeres appears to result from the patterned expression of several transcription factors and putative signaling molecules. We have applied a refined single-cell reverse transcription-polymerase chain reaction strategy to examine the molecular logic proposed to pattern the hindbrain at the single-cell level. This technique allows analysis of the concurrent expression of several genes within an individual cell at higher sensitivity than by *in situ* hybridization. Our results demonstrate that cells in rhombomere (r) 4 and r5 are heterogeneous in their expression of Hoxa-3, Hoxb-2, Sek-1, and Krox-20, suggesting that single cells are dynamically regulating their rhombomere-specific gene-expression profiles. Furthermore, the strong correlation between Sek-1 and Krox-20 expression at stage 12 was greatly diminished by stage 16, suggesting that the proposed interdependence of these two genes is present only at early stages of hindbrain development.

INTRODUCTION

Rhombomeres (r) are a series of morphologically distinct bulges that appear transiently in the vertebrate hindbrain (Lumsden and Keynes, 1989), which in chickens and mice separate the hindbrain into eight domains. With the formation of each rhombomere boundary, a polyclonal cell migration domain is established within which cells can intermix dramatically, but between which few cells pass (Birgbauer and Fraser, 1994; Fraser *et al.*, 1990). There is a strong correlation between this segmentation and the patterned expression of Hox-class homeobox genes (Hunt *et al.*, 1991; Murphy *et al.*, 1989; Murphy and Hill, 1991; Sundin and Eichele, 1990; Wilkinson *et al.*, 1989b), tyrosine kinase receptors such as Sek-1 (Gilardi-Hebenstreit *et al.*, 1992; Nieto *et al.*, 1992), and transcription factors such as Krox-20 (Chavrier *et al.*, 1988; Wilkinson *et al.*, 1989a) and *kreisler* (Cordes and Barsh, 1994). Such observations have led to the suggestion that some or all of these molecules play important roles in early patterning of the hindbrain.

Direct evidence for the roles of Hoxa-1, Hoxa-3, Krox-20, and others in the development of rhombencephalic and craniofacial structures has come from analyses of germ-line mutations in mice (Krumlauf, 1994; Schneider-Maunoury *et al.*, 1993). For example, disruption of Hoxa-1 (Lufkin *et al.*, 1991; Mark *et al.*, 1993) results in a hindbrain with only five distinct rhombomeres instead of the normal eight; in addition, motor neurons of the facial (VII) and abducens (VI) nerves are missing. Disruption of Hoxa-3 (Chisaka and Capecchi, 1991) displaces pharyngeal arch 4. Disruption of Krox-20 by germ-line mutation permits r3 and r5 to form, but results in the elimination or severe reduction of these rhombomeres at a later stage of the segmentation process, the severe reduction of motor nucleus of the trigeminal nerve (Vmn), and the disappearance of the abducens (VI) nerve, which normally differentiate from r2–r3 and r5–r6, respectively (Schneider-Maunoury *et al.*, 1993; Swiatek and Gridley, 1993).

Understanding the molecular hierarchies that result in hindbrain segmentation requires knowledge of the interactions between the Hox genes, Sek-1 and Krox-20. Several lines of evidence suggest that Krox-20 is an upstream regulator of a number of genes important for the establishment, consolidation, or maintenance of rhombomeres. For exam-

[1] Present address: Nara Institute of Science and Technology, 8916-5 Takayama, Ikoma, Nara 630-01, Japan.

0012-1606/97 $25.00

ple, the overlapping expression patterns of Krox-20 with Sek-1, Hoxa-2, and Hoxb-2 in r3 and r5, and with Sek-1, Hoxa-3, and Hoxb-3 in r5 (Krumlauf, 1993; Nieto *et al.*, 1992), led to the suggestion that these three genes are targets for Krox-20. In addition, analyses of the *cis*-regulatory domain of Hoxb-2 reveal binding sites for Krox-20 within an evolutionarily conserved r3/r5 enhancer that can drive regional expression of reporter genes in transgenic mice, demonstrate that the region-specific expression is lost if Krox-20 binding sites are mutated, and establish that ectopic expression of Krox-20 in transgenic mice can ectopically activate the r3/r5 enhancer (Sham *et al.*, 1993; Nonchev *et al.*, 1996, Vesque *et al.*, 1996). Such data, in combination with that from Hox gene expression studies in Krox-20 null mice (Schneider-Maunoury *et al.*, 1993), have been taken as evidence that Krox-20 is a direct activator that is both sufficient and necessary for the regional expression of some genes in the hindbrain. Slight differences in the time courses of expression for some of the genes in r3 and r5 might suggest that their relationship might vary with stage or position. However, the combination of genes expressed in individual cells during the formation of rhombomeres can only be inferred from comparing the results of *in situ* hybridization between different specimens. Because most of these gene products act exclusively within the cells that express them, this critical gap in our knowledge leaves questions of the molecular regulation of hindbrain segmentation unanswered. Here, we report the use of an approach capable of examining the coexpression of several mRNAs (Ruano *et al.*, 1995) to detect transcripts of four Hox genes, Sek-1, and Krox-20 within single cells of the chick hindbrain. The patterns of transcripts within single cells offers evidence for both changes and heterogeneity in gene expression at different developmental stages.

MATERIALS AND METHODS

In Situ Hybridization

White Leghorn chick embryos were incubated at 38°C and staged according to the criteria of Hamburger and Hamilton (1951). *In situ* hybridization was performed on whole mounts of stage 12 (15 to 18 somites) and 16 (26 to 28 somites) embryos as previously described (Wilkinson, 1992). After staining, embryos were examined under a microscope and digital images captured using a Roche ProgRes camera and Image Manager software (Roche Image Analysis Systems, Inc.). Digoxigenin-labeled antisense riboprobes were prepared according to the manufacturer's instructions (Boehringer Mannheim) by reverse transcription of DNA templates subcloned into pBluescript (Stratagene) or pGEM-4 (Promega). The probe for Hoxb-4 was synthesized from a 1176-bp full-length cDNA (Sasaki and Kuroiwa, 1990), Hoxa-3 was from a 930-bp genomic clone (Saldivar *et al.*, 1996), and Hoxb-2 was from a 700-bp genomic clone (C. Vesque *et al.*, submitted). Krox-20 represented a 150-bp cDNA fragment encoding the zinc finger domain (Nieto *et al.*, 1991) and Sek-1 was from a 417-bp cDNA fragment (Sajjadi and Pasquale, 1993).

Isolation of Total RNA and PCR Analysis

Total RNA was isolated by the one-step procedure (Chomczynski and Sacchi, 1987) using RNAzol (Teltest, Inc.) from pools of r4, r5, or r7/8/spinal cord tissue, harvested from 8–12 stage 16 chick embryos and its concentration determined by measuring adsorption at 260 nm (Sambrook *et al.*, 1989). Total RNA (1 μg to 0.1 pg) was reverse transcribed using 100 units MMLV reverse transcriptase (GIBCO BRL), 200 ng random hexonucleotide primers (Promega), 0.5 mM dNTP (Pharmacia-LKB) in the buffer supplied by the manufacturer and reaction volume of 10 μl at 37°C for 1 h.

Several target sequences were simultaneously amplified from a single cDNA synthesis by multiplex PCR using nested primers and two rounds of amplification. For the first round of amplification, cDNA synthesized from total RNA was amplified for 35 cycles [0.5–1 min, 94°C; 1–2 min, 55—65°C (depending on primer combination); 1.5–2 min, 72°C] in a 50-μl reaction containing up to four pairs of outside primers (0.2 μM final concentration), $MgCl_2$ (1.5 mM), dNTPs (0.2 mM), and *Taq* polymerase (1.25 unit; Promega) in the buffer supplied with the enzyme in a DNA thermal cycler (Model 9600; Perkin–Elmer Cetus). Subsequently, first-round PCR products were diluted 1000-fold and reamplified for 35 cycles in separate reactions using the corresponding internal primer pairs for each template. PCR products were labeled by inclusion of approximately 2×10^5 cpm of ^{32}P-labeled forward primer in each reaction. In some experiments gels were also stained with ethidium bromide and scored for the presence of PCR product. The identities of the PCR fragments from total RNA were confirmed by direct sequencing: sequence of Hoxb-4, Hoxa-3, Hoxb-2, Hoxb-1, and Sek-1 fragments resulting from transcripts were identical with known sequences. The sequence of the Krox-20 fragment (Nieto *et al.*, 1991) showed a single point mutation that did not alter the open reading frame.

Single-Cell PCR Analysis

Hindbrains were dissected from stage 12 and stage 16 chick embryos and pinned out in a Sylgard 182 (Dow Corning Corp.)-coated dish filled with Howard's Ringer solution (0.81 mM Na_2HPO_4, 123 mM NaCl, 1.56 mM $CaCl_2$, 4.96 mM KCl, pH 7.4). Pieces of tissue from r4 or r5 were isolated from three or four embryos by aspiration with a fire-polished pipette. Tissues were incubated in papain (5 min at 37°C in 2 units; Worthington Biochemical Corp.) in 15 μl of Hepes buffered saline (0.17 mM Na_2HPO_4, 0.22 mM KH_2PO_4, 137 mM NaCl, 5.36 mM KCl, 9.85 mM Hepes, 33.3 mM glucose, 43.8 mM sucrose, pH 7.4), washed twice in saline, dispersed by trituration through a fire-polished glass micropipette, and plated into 100-μl drops of L15 medium containing 10% heat-inactivated horse serum, on poly-D-lysine (Collaborative Biomedical Products)-coated glass coverslips. After the cells were allowed to adhere for 5–10 min at room temperature, coverslips were flooded with additional medium and stored at room temperature for up 3 h before use.

The procedure used for harvesting the contents of single cells using whole-cell patch-clamp pipettes has been described previously (Smith and O'Dowd, 1994; O'Dowd *et al.*, 1995). Briefly, coverslips were transferred to a recording chamber and perfused with an external medium containing 140 mM NaCl, 4 mM $MgCl_2$, 3 mM KCl, 1 mM $CaCl_2$, and 5 mM Hepes, pH 7.2, 290 mOsmol/kg. High-resistance seals were formed with the cell membranes of clearly separated individual cells using whole-cell patch-clamp recording pipettes filled with 20 mM NaCl, 120 mM potassium

gluconate, 2 mM $MgCl_2$, 0.1 mM $CaCl_2$, and 10 mM Hepes, pH 7.2, 280–283 mOsmol/kg. Recording pipettes were unpolished with open pipette resistances of 4–6 MΩ. Following formation of a high-resistance seal, the patch of membrane under the electrode tip was ruptured and the contents of the cell were aspirated into the pipette and transferred to a microfuge tube containing the first-strand cDNA synthesis premix (Smith and O'Dowd, 1994; O'Dowd *et al.*, 1995). First-strand cDNA synthesis was initiated by the addition of 100 units of MMLV reverse transcriptase followed by incubation for 1 h at 37°C. The reaction mixture was denatured at 95°C for 5 min and target cDNA templates were amplified by multiplex PCR as described above. The identity of each PCR product was confirmed by restriction mapping with two different enzymes, yielding the expected fragment sizes.

PCR Primers

Nested primers used for the PCR analyses were selected based on the known chick cDNA or genomic sequences and are given here. The outside primer pair is listed first in each case; the size of the final amplification product is shown in parentheses: Hoxb-4 (Sasaki and Kuroiwa, 1990), 5′-CATGAGCTCGTTTTTGATCA-3′/3′-AGAAGTCCCCTTTATTATTA-5′ and 5′-TCCAACATGAAGCGATGTAC-3′/3′-TGTTCAATGGGTTGTGGTTC-5′ (509 bp); Hoxa-3 (Saldivar *et al.*, 1996), 5′-CATGATGACCTCTTCAGGAG-3′/3′-ACCCTTAGGTGTATATGTCC-5′ and 5′-ACCTAAACTCTATGCATTCT-3′/3′-GACTTATGCTATGAGTAGGA-5′ (191 bp); Hoxb-2 (Vesque *et al.*, 1996), 5′-TTTAACACACGCAGGGGTTG-3′/3′-TTGTGTCATGTTTCTTGGGG-5′ and 5′-CTGGAGCTGGAGAAGGAATT-3′/3′-TTTCACACCAAGGTCTTGGC-5′ (116 bp); β-actin (Kost *et al.*, 1983), 5′-TGGATGATGATATTGCTGCG-3′/3′-ACTATACCTCTTCTAGACCG-5′ and 5′-CTGTGTTCCCATCTATCGTG-3′/3′-CTTGTGCCATAACAGTGGTT-5′ (148 bp); Hoxb-1 (Sundin *et al.*, 1990), 5′-TAAATGAGGACAAAGACCCC-3′/3′-TGTCTTCTTCTCCCTTTTCC-5′ and 5′-GATGAAAGTGAAGAGGAACC-3′/3′-GAGTTGCTTTGGGTTCAGTT-5′ (201 bp); Sek-1 (Sajjadi and Pasquale, 1993), 5′-AACGCAATGGTGAATGCCAA-3′/3′-GCTTCCAAAGGTAGTGACTG-5′ and 5′-ATACTACAAGGCGCTCTCAA-3′/3′-GTCACCACATGTAAAGTCGG-5′ (326 bp); and Krox-20 (Nieto *et al.*, 1991), 5′-TGCGACAGACGCTTCTCTCG-3′/3′-CCTGTGTGTGGCCGCTCTTC-5′ and 5′-GAACTGACCCGACACACCCGAAT-3′/3′-TCGCTGGTGAACTGGTGAGTGTA-5′ (101 bp).

RESULTS

To test the feasibility of a single-cell RT-PCR analysis, we compared the regional expression of three Hox genes, determined by *in situ* hybridization, RT-PCR from total RNA isolated from whole rhombomeres, and single-cell RT-PCR. In the rodent hindbrain, *in situ* hybridization studies have demonstrated that Hoxa-3, Hoxb-2 and Hoxb-4 have unique but overlapping patterns of expression (Hunt *et al.*, 1991; Krumlauf, 1993; Wilkinson *et al.*, 1989b). We observed similar patterns of expression by *in situ* hybridization in the chick (Fig. 1). High levels of Hoxb-4 expression are present in spinal cord and in caudal hindbrain (r7 and r8) (Fig. 1A); the rostral boundary of Hoxa-3 is at the r4/r5 border (Fig. 1B). However, in contrast to the pattern of

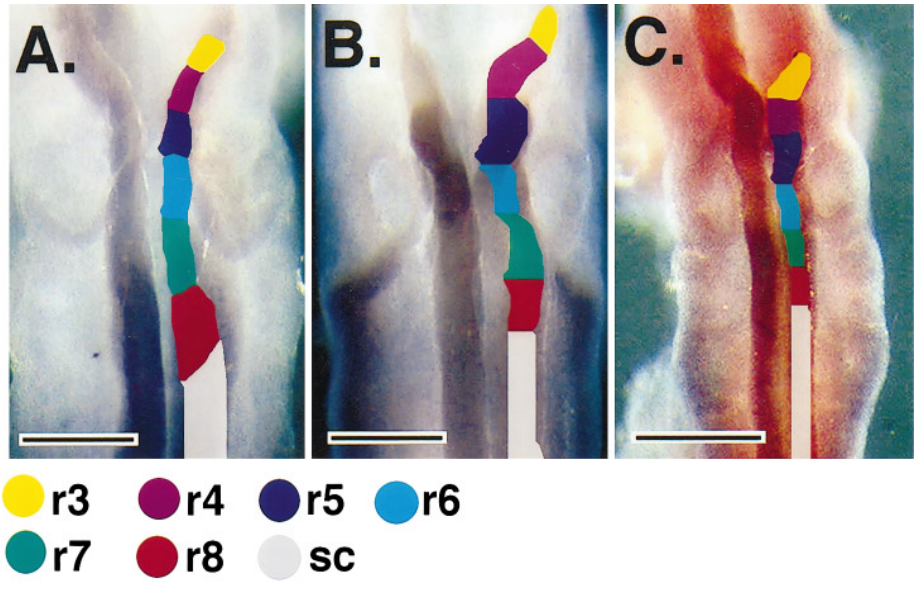

FIG. 1. Hox gene expression in chick hindbrain and spinal cord. Dorsal view of whole-mount stage 16 chick embryos hybridized with antisense digoxigenin-labeled riboprobes for (A) Hoxb-4 (26-somite stage; 26ss), (B) Hoxa-3 (28ss), and (C) Hoxb-2 (25ss). High levels of Hoxb-4 are observed in r7, r8, and spinal cord (A); Hoxa-3 expression is seen in r5 and more caudal regions (B). High levels of Hoxb-2 expression are present in r4 and r7 to r8. The positions of the rhombomeres are indicated by the color coding on the right side of each embryo. Scale bar, 200 μm.

expression in mouse, where Hoxb-2 mRNA expression is high in r3, r4, and r5 (Wilkinson *et al.*, 1989b), high levels of Hoxb-2 expression in chick were observed only in r4; expression in r3 was much lower (Fig. 1C).

Multiplex RT-PCR yields a pattern of gene expression that confirms and extends the *in situ* hybridization data. Multiple primers were used to simultaneously amplify specific target sequences in cDNA synthesized from total RNA isolated from different regions of the hindbrain. PCR products generated from r4, r5, and spinal cord RNA were of sizes predicted for each target sequence (Hoxa-3, Hoxb-2, Hoxb-4, and β-actin; Fig. 2A); their identities were confirmed by sequencing. β-Actin primers, included as a positive control, were effective in amplifying RNA isolated from all three regions. Consistent with the *in situ* analysis, Hoxb-4 mRNA was present in RNA isolated from spinal cord, but not in RNA isolated from more rostral rhombomeres (r4 and r5). However, based on the results of the *in situ* hybridization experiments, Hoxa-3 RNA, which was expected to be present only in the samples from r5 and spinal cord, was also found in RNA isolated from r4. Hoxb-2 expression, which was expected in r4 and spinal cord, was also present in r5. To determine whether these differences might result from the higher sensitivity of the PCR technique, we examined the quantitative differences between the levels of expression in r4 and r5. To obtain a measure of the relative amounts of transcript for a given gene, we determined the frequency of positive polymerase chain reactions as a function of the amount of input RNA isolated from r4 and r5 used for the first-strand cDNA synthesis (Figs. 2B, 2C, and 2D). Each of these data sets was well fit by the equation for an absorption isotherm, and these fits were used to determine the effective concentration of total RNA necessary for a positive PCR in 50% of the cases (EC_{50}). As expected for a highly expressed, ubiquitous marker such as β-actin, a low EC_{50} of 0.002 ng total RNA was obtained for both r4 and r5 (Fig. 2B). In contrast, the EC_{50} for Hoxa-3 was 6.2 ng total RNA for r4, compared with 0.76 ng for r5, suggesting that the concentration of Hoxa-3 template is approximately eightfold lower in r4 than in r5 (Fig. 2C). The EC_{50} of Hoxb-2 was four to five times lower for r5 than for r4 (Fig. 2D). Thus, the higher sensitivity of the RT-PCR extends the *in situ* analysis by showing that the apparent boundaries in gene expression between adjacent rhombomeres are quantitative rather than qualitative.

Finally, we compared the patterns of expression of these same Hox genes using single-cell RT-PCR. Pieces of tissue were dissected from r4 and r5 (Fig. 3A), dissociated by brief enzymatic treatment, and dispersed onto glass coverslips, yielding single cells 5–15 μm in diameter (Fig. 3B). Clearly separated cells were identified visually; glass micropipets were used to form gigaohm seals on the cells and to then aspirate their contents. Electrophysiological recording obtained from some cells prior to harvesting the cytoplasm revealed the presence of voltage-gated outward currents (data not shown). The results of a typical multiplex RT-PCR experiment, examining the coexpression of Hoxa-3, Hoxb-2, Hoxb-4, and β-actin in single cells, are shown in Fig. 3C (lanes 1–28). Consistent with the RT-PCR analysis of RNA isolated from each rhombomere, the amplified product for β-actin was present in all cells from both r4 and r5, but was absent in samples of culture medium bathing the cells (sampled four times over the course of the experiment; Fig. 3C, lanes labeled M). Moreover, no Hoxb-4 PCR product was detected in any of these cells, suggesting that the level of contamination by cells from rhombomeres outside of r4 and r5 was minimal. Rhombomere-specific differences, however, were apparent in the frequency of cells expressing Hoxa-3 and Hoxb-2 (Fig. 3C and Table 1). In agreement with the finding from total RNA RT-PCR analysis, the frequency of expression of Hoxa-3 is five times higher in r5 than in r4 ($P < 0.001$, by a z test of proportions), whereas the frequency of Hoxb-2-positive cells was only slightly higher in r4 than in r5. Some cells in both r4 and r5 expressed both Hoxa-3 and Hoxb-2.

These initial experiments demonstrate that mRNA encoding at least two Hox genes can be amplified from single cells. Furthermore, the ensemble average of the single-cell data both confirms and extends previous total RNA and *in situ* hybridization data. In particular, the quantitative difference between Hoxa-3 expression in r4 vs r5 (Fig. 2B) appears to result from a low percentage of Hoxa-3-positive cells in r4.

Coexpression of Krox-20 and Sek-1 Is Developmentally Regulated

Previous studies have suggested regulatory interaction between Krox-20 and several other genes, including Hoxb-2 (Sham *et al.*, 1993; Nonchev *et al.*, 1996; Vesque *et al.*, 1996) and Sek-1 (Nieto *et al.*, 1992; D. G. Wilkinson, pers. comm.), that are thought to be important in the metameric organization of the early hindbrain. Consistent with this hypothesis, *in situ* hybridization in chick at stage 12 shows high levels of expression of both Krox-20 and Sek-1 in r3 and r5, but much lower levels in the intervening r4 (Figs. 4A and 4C). A similar overlapping pattern of expression of these two genes is seen at stage 16 (Figs. 4B and 4D).

To examine the potential interactions between Krox-20 and Sek-1, as well as some of their potential targets, we used multiplex RT-PCR of single cells from r5 to determine the frequency of coexpression of Krox-20, Sek-1, Hoxb-1, and Hoxb-2. To minimize the chances of contamination of cells from other rhombomeres, our dissection of r5 cells was confined to a 100-μm-diameter zone in the middle of the intermediate region of r5. Although this region has the disadvantage of lower Krox-20 expression, it eliminates the possibility of contamination from neural crest cells, which cross rhombomere boundaries in the more dorsal regions of the hindbrain (Birgbauer *et al.*, 1995). The results of a typical experiment from cells at stage 16 are illustrated in Fig. 5. PCR products representing one or more of the target mRNAs were successfully amplified from the majority of the cells. Table 2 summarizes the results obtained from five experiments on stage 12 or stage 16 embryos. Note that the

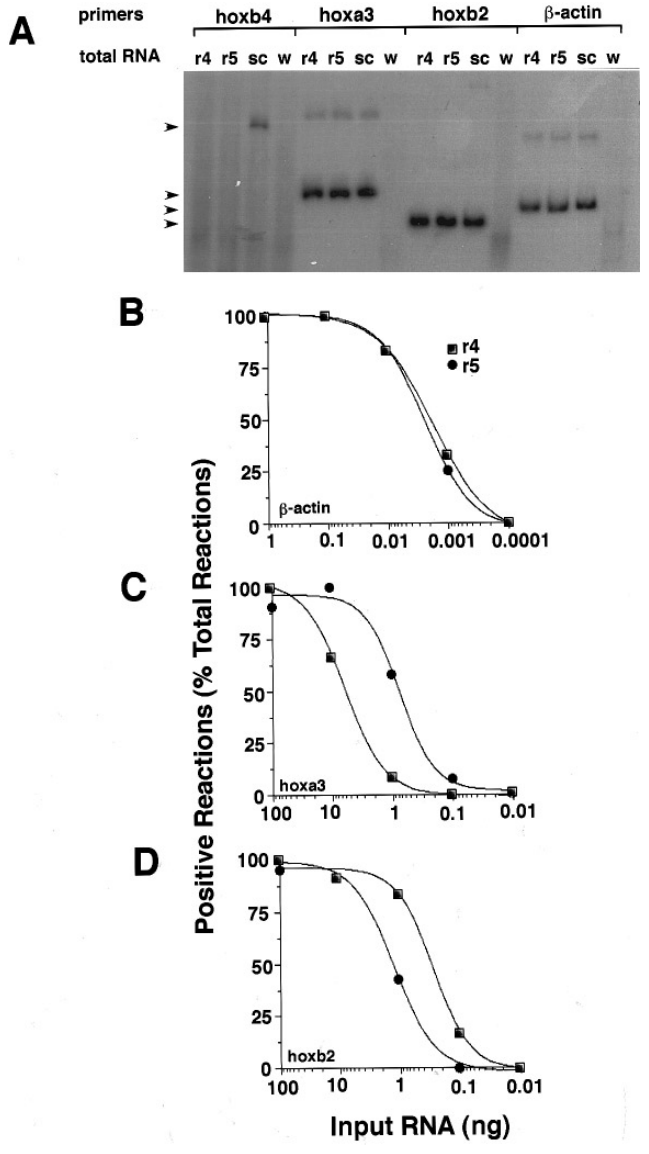

FIG. 2. Multiplex RT-PCR of total RNA. (A) The patterns of expression of Hoxb-4, Hoxa-3, Hoxb-2, and β-actin were examined in 1 μg total RNA isolated from r4, r5, and spinal cord from stage 16 chick embryos by multiplex PCR. PCR products representing Hoxa-3 (190 bp), b2 (115 bp), and β-actin (147 bp) transcripts are present in tissue obtained from all three areas, whereas Hoxb-4 (508 bp) is detected only in spinal cord. No products are amplified when water (w) is used in place of total RNA during the cDNA synthesis. Arrowheads mark the expected sizes of fragments derived from Hoxb-4, Hoxa-3, β-actin, Hoxb-2, from top to bottom. (B, C, and D) To determine the relative concentration of mRNA encoding β-actin, Hoxa-3, and Hoxb-2 in total RNA isolated from r4 and r5, we determined the limiting dilution for each. Twelve multiplex polymerase chain reactions were performed at a variety of concentrations of RNA used for the initial cDNA synthesis, and the fraction of reactions for which an amplified product was obtained was determined. The curves were fit by a simple absorption isotherm equation (r^2 values > 0.99) and the EC_{50} values determined. Comparison of these values indicates that, in contrast to the similar levels of β-actin RNA in the two rhombomeres, Hoxa-3 is expressed at significantly higher levels in r5 (8-fold) and Hoxb-2 at higher levels in r4 (4.6-fold).

frequency of successful amplification for each of the four genes was similar at the two stages. The single cells appear to have a molecular identity appropriate for their r5 origin, as the patterns of gene expression are consistent with our RT-PCR analysis of whole rhombomere RNA (data not shown) and with *in situ* hybridization studies (Fig. 1; Sundin and Eichele, 1990).

Multiplex PCR was used to examine the patterns of gene coexpression at the single-cell level (cf. Fig. 5A). In two independent experiments performed at stage 12, the expression of Krox-20 was strongly correlated with Sek-1, with 80% of the Krox-20-positive cells also expressing Sek-1. By stage 16, this correlation had decreased dramatically; only a small fraction of the Krox-20-positive cells were positive for Sek-1 (11%) in three independent experiments. This was not due to a change in the assay conditions with developmental age, as the correlation between Hoxb-2- and Sek-1-positive cells remained constant, at about 75%, between stages 12 and 16 (Fig. 5B). Similarly, the low probability of detecting Krox-20 in Hoxb-2-positive cells changed little with development. Thus, while the percentage of cells expressing either Sek-1 or Krox-20 did not change during development (Table 2), the fraction of Krox-20-positive cells that coexpress Sek-1 changed dramatically ($P < 0.02$ by a z test of proportions; Fig. 5B).

Potential for False-Negative and False-Positive Results

The strength of these data rest, in part, on an assumption that the assay is of high fidelity, giving no PCR product if the cell lacks the transcript under study (i.e., no false positives) and successfully amplifying the target sequence for all cells that contain the transcript (i.e., no false negatives). The assay does not appear to be prone to false positives, a potential problem given the many cycles of PCR amplification. Contaminating templates in the medium, equipment, or reagents are easily detected by interleaved control experiments in which PCR amplification was performed on water or the medium bathing the cells (Figs. 3 and 5, lanes marked W or M). Experiments in which any of these negative control lanes were positive were discarded. Contamination from genomic DNA also seems unlikely. Even when nuclei are harvested intentionally, genomic templates are not amplified (Johansen *et al.*, 1995). Moreover, amplification of genomic templates would not be consistent with the distinct rhombomere-specific patterns of gene expression that we observe here. Finally, based on the size of the PCR product, primers for β-actin that span an intron demonstrate

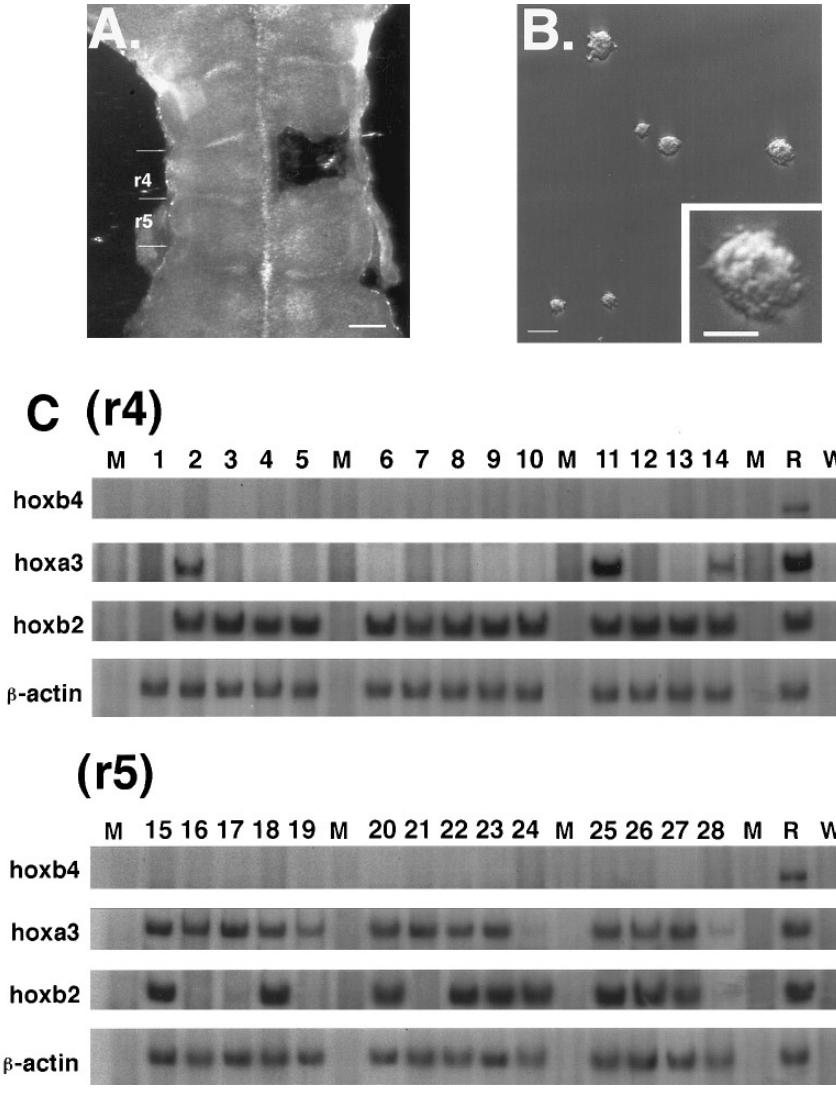

FIG. 3. Single-cell multiplex RT-PCR analysis of Hoxb-4, Hoxa-3, Hoxb-2, and β-actin. (A) Dorsal view of a flattened hindbrain from stage 16 chick embryo from which r4 on the right-hand side has been removed. (B) Single cells of 5–15 μm in diameter, isolated from r4 at stage 16, plated on poly-D-lysine-coated coverslip. (C) Multiplex RT-PCR from single cells isolated from r4 or r5. Products from one or more target sequences were amplified from individual cells (lanes 1–28). In contrast, no products were amplified when either medium bathing the cells (M) or water (W) was used in place of the cell extract in the first-strand synthesis. Lane R presents the RT-PCR products for each gene (Hoxb-4, Hoxa-3, Hoxb-2, and β-actin) from total RNA of r7/r8/spinal cord. Scale bar, 100 μm in A, 20 μm in B, and 10 μm in the inset.

that the major amplified species resulted from mature mRNA (data not shown).

We can also be confident that our data are not contaminated by template sequences present in cells from rhombomeres other than r4 or r5. In the initial experiments, we examined the expression of Hoxb-4 to address this issue. Although Hoxb-4 is present at high levels in r7-spinal cord, we were never able to amplify Hoxb-4 from single cells isolated from either r4 or r5, suggesting that cells from the more caudal regions did not contaminate these preparations. In the second series of experiments, in which we focused our analysis on expression of genes in r5, dissections were confined to the central region of the rhombomere to reduce the possibility of inadvertently harvesting cells from adjacent rhombomeres. To identify potential contamination of these r5 cells, we tested the single cells for the expression of Hoxb-1, which is expressed at relatively high levels in r4. No expression was detected.

Finally, to assess the possible contribution made by false-negative results to our data, we examined the frequency with which identical PCR products could be amplified from cDNA obtained from single cells split between two independent poly-

TABLE 1

Frequency of Cells Expressing Hoxb-4, Hoxa-3, Hoxb-2, or β-Actin Genes

	No. of cells analyzed	β-actin	Hoxb-4	Hoxa-3	Hoxb-2	Hoxa-3 and Hoxb-2
r4	28	100%	0%	18%*	86%†	18%*
r5	28	100%	0%	89%	68%	64%

Note. Single-cell RT-PCR was performed as in Figs. 3C and D. Values presented are the percentage of cells dissociated from rhombomeres 4 or 5 at stage 16 that expressed a given mRNA or combination of mRNAs.

* $P < 0.001$, † $P \approx 0.1$ by a z test of proportions.

merase chain reactions. The number of cells in which the sister reactions were both positive (coherent positives) or both negative (coherent negatives) or in which one reaction was positive and the other negative (incoherent) was determined. In one such experiment, in which the cDNA from 14 cells was split in two, the majority of cells were coherent positives for Sek-1 and coherent negatives for Krox-20 (Table 3), and the number of incoherent reactions for these two genes were both small (2/14). The small fraction of incoherent cases suggests that the false-negative rate is relatively low. A quantitative estimate of the expected rate of false negatives can be made from the fraction of incoherent positive RT-PCR samples (Table 3) and suggests that the false-negative rate should be less than 10% (estimated at 1% for Sek-1; 7% for Krox-20). Thus, false negatives should not significantly influence our determination of the frequency of Sek-1 (42%)- or Krox-20 (82%)-negative cells.

DISCUSSION

The vertebrate hindbrain has served as an important testing ground for mechanisms of brain regionalization. The

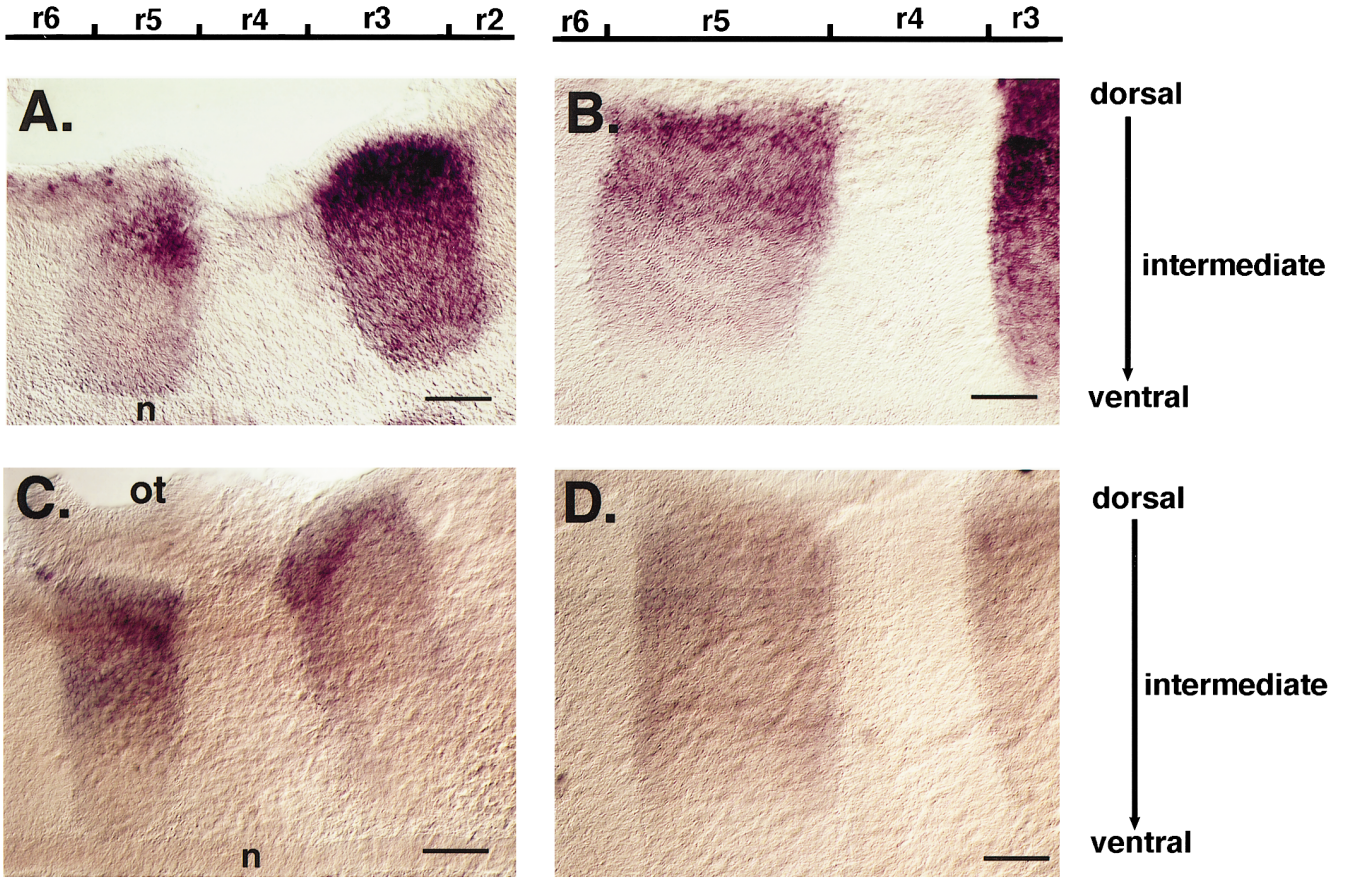

FIG. 4. *In situ* hybridization demonstrates overlapping pattern of Sek-1 and Krox-20 expression in chick hindbrain. Flattened whole mounts of hindbrains dissected from chicken embryos following hybridization of the whole embryos with antisense riboprobes. Expression levels of Sek-1 [(A) stage 12, (B) stage 16] and Krox-20 [(C) stage 12, (D) stage 16] are high in r3 and r5, but low in r4. Note the gradation in expression levels, with the highest expression in the dorsal regions of the rhombomere. Cells were harvested from the 100-μm diameter region in the middle of rhombomere 5. In all panels, dorsal is at the top and rostral is to the right. Letters denote the positions of the otic vesicle (ot) and notochord (n). Scale bar, 50 μm.

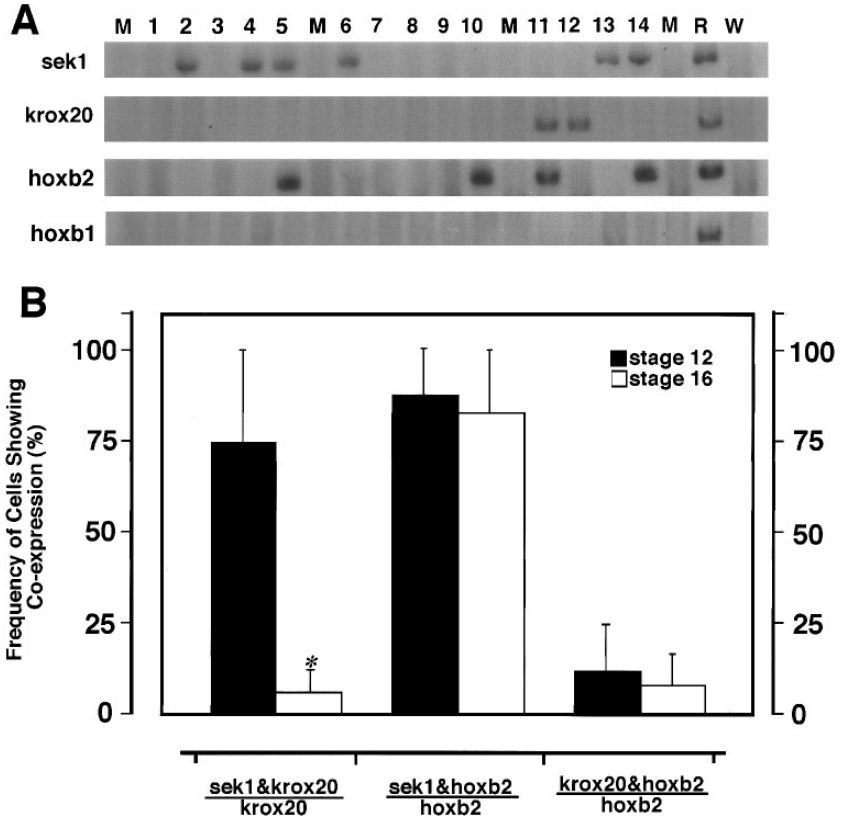

FIG. 5. Coexpression of Sek-1 and Krox-20 in single cells is developmentally regulated. (A) Autoradiograms of a single-cell multiplex PCR experiment analyzing coexpression of Krox-20, Sek-1, Hoxb-2, and Hoxb-1 in single cells isolated from r5 at stage 16. The majority of the cells (lanes 1–14) expressed one or more of the target genes (summarized in Table 2). PCR products representing all four target sequences were amplified from total RNA of r4 and r5 (lane R). No products were amplified when either medium bathing the cells (M) or water (W) was used in place of the cell extract in the first-strand synthesis. (B) The frequency with which a given gene was coexpressed with another was determined by single-cell multiplex RT-PCR. The number of Krox-20-positive cells that coexpress Sek-1 declined significantly between stage 12 (filled bars) and stage 16 (open bars). Whereas the majority of Hoxb-2-positive cells also expressed Sek-1, only a small fraction of Hoxb-2-positive cells expressed Krox-20 at both stages. Values presented are from two experiments at stage 12 and three experiments at stage 16 ($n = 14$ cells per experiment), error bars show SEM. * $P < 0.02$ (z test of proportions).

rhombomeres and their boundaries provide powerful and convenient landmarks for studies at both the molecular and the cellular level. Studies of the developing hindbrain at the cellular level rely on the ability to obtain single-cell resolution, yielding insights into cell lineages (Fraser *et al.*, 1990; Lumsden *et al.*, 1994) as well as the cell movements (Birgbauer *et al.*, 1994) that build the hindbrain. The goal of the experiments presented here was to refine and employ a molecular approach with single-cell resolution to explore the molecular mechanisms that underlie hindbrain patterning. Using multiplex RT-PCR, we demonstrate that it is possible to detect multiple transcripts in single cells with higher sensitivity than *in situ* hybridization, permitting direct analysis of the coexpression of four different genes in individual cells. Ensemble-averages of the single-cell data match well with the predictions from total RNA studies, suggesting that the technique can provide an accurate picture of gene expression patterns. The technique has a low false-negative rate (estimated here as less than 10%), and any experimental sessions in which false-positive results might be present are easily recognized and discarded. Thus, single-cell RT-PCR is suitable to test the operation of molecular logic systems at the single-cell level that has been suggested by previous tissue-level experiments.

The results presented here suggest that gene expression in the developing hindbrain is more heterogeneous than might be expected from previous studies. The resolution provided by *in situ* hybridization is adequate to determine the regional patterns of gene expression, resulting in a good understanding of hindbrain patterning at rhombomere levels of resolution. However, because the direct effects of receptors and transcription factors are restricted to the cells expressing them, cellular, not rhombomeric, resolution is required. Beyond showing cell-to-cell variations in the in-

TABLE 2

Frequency of Cells Expressing Hoxb-1, Hoxb-2, Sek-1, and Krox-20

	No. of experiments (cells analyzed)	Hoxb-1 %	Hoxb-2 %	Sek-1 %	Krox-20 %
Stage 12	2 (28)	0%	18 (±11)	58 (±21)	18 (±4)
Stage 16	3 (42)	0%	21 (±4)	48 (±9)	21 (±11)

Note. Single-cell RT-PCR was performed as described for Fig. 5. Dispersed cells, dissected from the intermediate area of approximately 100-μm diameter in r5, were subjected to single-cell RT-PCR. The fraction of cells expressing Hoxb-2 in this sample of r5 is lower than in Table 1, probably because the most dorsal area of r5 was not included in the dissociated region. The values do not add up to 100% because in some cases none of the target sequences amplified; in other cases more than one target sequence amplified. Reported values are mean ± standard error for two experiments at stage 12 and three experiments at stage 16 (14 cells for each experiment) except for Hoxb-1, for which only a single experiment of 14 cells was analyzed.

tensity of the reaction product, *in situ* hybridization leaves open most questions of heterogeneity and permits only deductions concerning the sets of genes that are expressed within any one cell. Multiplex RT-PCR demonstrates that individual cells express only a subset of the genes expected from their rhombomere of origin. For example, the majority of r4 cells expresses Hoxb-2 alone; other cells express both Hoxb-2 and Hoxa-3. It remains unknown if the heterogeneity observed at the stages examined here reflects differences either in the developmental histories of the cells (cf. Birgbauer *et al.*, 1994) or in their developmental fates, or merely stochastic variation in the gene expression. The greater sensitivity of the RT-PCR technique offers its own advantages; for example, it helps to resolve the apparent differences in the patterns in Hoxb-2 expression in chick and mouse, by demonstrating that the difference is quantitative rather than qualitative (Fig. 2).

We used the multiplex RT-PCR technique to begin a detailed examination of the relationship between Sek-1 and Krox-20. Based upon their temporal and spatial patterns of expression, these two genes have been proposed to play important roles in specifying each other's expression. By extending the analysis to the single-cell level, the results suggest there is not a fixed relationship between the expression of these two genes. Cells in r5 show an 80% correlation in their Sek-1 and Krox-20 expression early in the segmentation of the hindbrain (stage 12); however, only a day later (stage 16) the correlation between the expression of Sek-1

TABLE 3

Estimation of the Frequency of False Negatives in Single-Cell RT-PCR

	Coherent positive	Incoherent	Coherent negative	Observed negative	*P*	*r*	Theoretical false negative
Sek-1	9	2	3	43%	90%	79%	1%
Krox-20	1	2	11	82%	50%	29%	7%

Note. The reliability of the single-cell RT-PCR technique and the potential of false-negative results was tested by splitting the cDNA obtained from single cells into two independent polymerase chain reactions. If the technique is perfectly reliable, identical PCR products should be amplified from the two tubes. The fraction of cases in which the two tubes yield different (incoherent) results can be used to calculate the expected number of false-negative results when the PCR is performed without splitting into two tubes. The contents were harvested from 14 single cells from r5 at stage 12. After first-strand cDNA synthesis, the contents were split into duplicate tubes and otherwise processed identically to the previous samples using mixed primers for Hoxb-1, Hoxb-2, Sek-1, and Krox-20. Coherent positive (CP) is the number of cases in which PCR amplification took place in both tubes. Incoherent (I) is the number in which the amplification took place in only one of the two tubes. Coherent negative (CN) means both tubes were negative. Observed negative is the value obtained in two or three independent experiments of 14 cells each (data from Table 2). The distribution of these three cases will depend upon both the probability that the randomly selected cells contained the transcript(s) in question (defined as *r*) and the probability of successful PCR amplification of each of the tubes from cells that contained the relevant transcript (defined as *P*). The number of pairs of PCR tubes is given by *n*. Based on these definitions, three equations can be defined:

$$(\mathrm{CP}) = P^2 \times r \times n, \quad [1]$$

$$(\mathrm{I}) = 2 \times P \times (1 - P) \times r \times n, \quad [2]$$

$$(\mathrm{CN}) = [(1 - r) + (1 - P)^2 \times \mathrm{r}] \times n. \quad [3]$$

By inserting the values for CP, I, and CN from the table, three equations result that can be used to define values for the two unknowns (*r* and *P*). These values are presented as *r* and *P* in the table. The rate of theoretical false negatives expected when the cDNA is not split into two tubes can be predicted from the values of *r* and *P*, using Eq. [4].

$$\text{False negative rate} = (1 - P)^2 \times r. \quad [4]$$

Note that this is related to Eq. [3], which describes the fraction of coherent negative cases (in which neither PCR tube contained an amplified product). If the contents of the tubes was not split, the fraction $(1 - r)$ would be expected to be negative because that fraction of the cells does not express the target RNA (true positives); the remaining set of negative cases (by definition, false-negative cases), in which cells that actually contain transcript fail to amplify, is given by Eq. [4].

and Krox-20 had dropped precipitously to 11%. Interestingly, this decrease takes place during stages of development in which the regional patterns of gene expression appear to become more tightly regulated. This change does not reflect a dramatic down-regulation of either gene, and other genes remain constantly correlated (or uncorrelated) during the same time period. Given that proteins may outlive their mRNAs, it is not surprising to see Sek-1 expression in the absence of Krox-20. However, the lack of Sek-1 expression in cells expressing Krox-20 suggests either that translation of Krox-20 mRNA is blocked or that Krox-20 alone is not sufficient to drive Sek-1 transcription. Thus it appears that the molecular interactions proposed for Krox-20 and Sek-1 are likely to be involved in the initial patterning of the gene expression but may not be necessary for the maintenance of this pattern.

The multiplex RT-PCR also offers some insights into the relationship between Hoxb-2 and Krox-20 within single cells. At both stage 12 and stage 16 there is little if any correlation between Hoxb-2 and Krox-20, although there is a strong correlation between Hoxb-2 and Sek-1 (Fig. 5B). Functional Krox-20 binding sites are required for the activity of a r3/r5 enhancer, isolated from both chicken and mouse, when introduced as a reporter construct into transgenic mice (Nonchev *et al.*, 1996), suggesting that Krox-20 may be necessary for Hoxb-2 expression in r5. The weak correlation observed here suggests that Krox-20 might be neither sufficient nor necessary for Hoxb-2 transcription when the entire *cis*-regulatory domain is allowed to act in its normal context.

In summary, the experimental approach presented here offers the opportunity to test directly proposed mechanisms of gene control. Molecular interactions predicted from *in vitro* DNA binding studies or from the spatiotemporal patterns of gene expression can be examined within the context of single cells. These first results demonstrate that the interrelationships between genes may vary at the single-cell level much more than might be expected from tissue-level data. The technology is well suited for examining the molecular responses of cells that cross rhombomere boundaries within the neuroepithelium (Birgbauer and Fraser, 1994) or within the neural crest (Birgbauer *et al.*, 1995). When combined with technologies for misexpressing genes (cf. Kato *et al.*, 1994), experimental questions previously performed only in transgenic mice become practical in the experimentally accessible chicken embryo. Thus, the results presented here provide a molecular tool with single-cell precision that can be combined with cellular tools to better define the events of embryonic patterning in the vertebrate hindbrain and elsewhere.

ACKNOWLEDGMENTS

We thank Dr. Robb Krumlauf and Dr. David Wilkinson for their helpful advice and for providing probes for *in situ* hybridization studies. We also thank Dr. E. Davidson, Dr. D. Crotty, and Dian De Sha for critically reading the manuscript; M. D. Flowers, Dr. G. R. Belford, R. Colburn, and Dr. Yinong Zhang for technical assistance; and Dr. Yoshi-hisa Kubota for providing advice on statistical analysis. This work was supported by grants from the International Human Frontier Science Program (LT-186/94) to K.K., NSF Grant IBN-9319355 to M.A.S., and NIH Grants MH49176 and AR47671 to S.E.F., NS27501 and NS30109 to D.K.O'D., and NS33213 to M.A.S.

REFERENCES

Birgbauer, E., and Fraser, S. E. (1994). Violation of cell lineage restriction compartments in the chick hindbrain. *Development* **120,** 1347–1356.

Birgbauer, E., Sechrist, J., Bronner-Fraser, M., and Fraser, S. (1995). Rhombomeric origin and rostrocaudal reassortment of neural crest cells revealed by intravital microscopy. *Development* **121,** 935–945.

Chavrier, P., Zerial, M., Lemaire, P., Almendral, J., Bravo, R., and Charnay, P. (1988). A gene encoding a protein with zinc fingers is activated during G0/G1 transition in cultured cells. *EMBO J.* **7,** 29–35.

Chisaka, O., and Capecchi, M. R. (1991). Regionally restricted developmental defects resulting from targeted disruption of the mouse homeo-box gene *Hox1.5*. *Nature* **350,** 473–479.

Chomczynski, P., and Sacchi, N. (1987). Single-step method of RNA isolation by acid guanidinium thiocyanate phenol chloroform extraction. *Anal. Biochem.* **162,** 156–159.

Cordes, S. P., and Barsh, G. S. (1994). The mouse segmentation gene *kr* encodes a novel basic domain–leucine zipper transcription factor. *Cell* **79,** 1025–1034.

Fraser, S., Keynes, R., and Lumsden, A. (1990). Segmentation in the chick embryo hindbrain is defined by cell lineage restrictions. *Nature* **344,** 431–434.

Gilardi-Hebenstreit, P., Neito, M. A., Frain, M., Mattéi, M.-G., Chestier, A., Wilkinson, D. G., and Charnay, P. (1992). An Eph-related receptor protein tyrosine kinase gene segmentally expressed in the developing mouse hindbrain. *Oncogene* **7,** 2499–2506.

Guthrie, S., and Lumsden, A. (1991). Formation and regeneration of rhombomere boundaries in the developing chick hindbrain. *Development* **112,** 221–229.

Guthrie, S., Muchamore, I., Kuroiwa, A., Marshall, H., Krumlauf, R., and Lumsden, A. (1992). Neuroectodermal autonomy of Hox-2.9 expression revealed by rhombomere transpositions. *Nature* **356,** 157–159.

Hamburger, V., and Hamilton, L. (1951). A series of normal stages in the development of the chick embryo. *J. Morphol.* **88,** 49–92.

Hunt, P., Gulisano, M., Cook, M., Sham, M.-H., Faiella, A., Wilkinson, D., Boncinelli, E., and Krumlauf, R. (1991). A distinct *Hox* code for the branchial region of the vertebrate head. *Nature* **353,** 861–864.

Irving, C., Nieto, A., Dasgupta, R., Charnay, P., and Wilkinson, D. G. (1996). Progressive spatial restriction of Sek-1 and Krox-20 gene expression during hindbrain segmentation. *Dev. Biol.* **173,** 26–38.

Johansen, F. F., Lamobolez, B., Audinat, E., Bochet, P., and Rossier, J. (1995). Single cell RT-PCR proceeds without the risk of genomic DNA amplification. *Neurochem. Int.* **26,** 239–243.

Kato, K., Yoneda, Y., Okada, Y., Kiyama, H., and Shiosaka, S. (1994). Gene transfer and the expression of a foreign gene *in vivo* in postmitotic neurons of the adult rat brain using the hemagglutinating

virus of the Japan-liposome method. *Mol. Brain Res.* **25,** 359–363.

Kost, T. A., Theodorakis, N., and Hughes, S. H. (1983). The nucleotide sequence of the chick cytoplasmic beta-actin gene. *Nucleic Acids Res.* **11,** 8287–8301.

Krumlauf, R. (1993). *Hox* genes and pattern formation in the branchial region of the vertebrate head. *Trends Genet.* **9,** 106–112.

Krumlauf, R. (1994). *Hox* genes in vertebrate development. *Cell* **78,** 191–201.

Lufkin, T., Dierich, A., LeMeur, M., Mark, M., and Chambon, P. (1991). Disruption of the *Hox-1.6* homeobox gene results in defects in a region corresponding to its rostral domain of expression. *Cell* **66,** 1105–1119.

Lumsden, A., Clarke, J. D. W., Keynes, R., and Fraser, S. (1994). Early phenotypic choices by neuronal precursors, revealed by clonal analysis of the chick embryo hindbrain. *Development* **120,** 1581–1589.

Lumsden, A., and Keynes, R. (1989). Segmental patterns of neuronal development in the chick hindbrain. *Nature* **337,** 424–428.

Mark, M., Lufkin, T., Vonesch, J.-L., Ruberte, E., Olivo, J.-C., Dollé, P., Gorry, P., Lumsden, A., and Chambon, P. (1993). Two rhombomeres are altered in *Hox-a1* mutant mice. *Development* **119,** 319–338.

Murphy, P., Devidson, D. R., and Hill, R. E. (1989). Segment-specific expression of a homeobox-containing gene in the mouse hindbrain. *Nature* **341,** 156–159.

Murphy, P., and Hill, R. E. (1991). Expression of the mouse *labial*-like homeobox-containing genes, *Hox 2.9* and *Hox 1.6*, during segmentation of the hindbrain. *Development* **111,** 61–74.

Nieto, M. A., Bradley, L. C., and Wilkinson, D. G. (1991). Conserved segmental expression of *Krox-20* in the vertebrate hindbrain and its relationship to lineage restriction. *Development* **Suppl. 2,** 59–62.

Nieto, M. A., Gilardi-Hebenstreit, P., Charnay, P., and Wilkinson, D. G. (1992). A receptor protein tyrosine kinase implicated in the segmental patterning of the hindbrain and mesoderm. *Development* **116,** 1137–1150.

Nonchev, S., Maconochie, M., Vesque, C., Arparicio, S., Ariza-McNaughton, L., Mananares, M., Maruthainar, K., Kuroiwa, A., Brenner, S., Charnay, P., and Krumlauf, R. (1996). The conserved role of Krox-20 in directing Hox gene expression during vertebrate hindbrain segmentation. *Proc. Natl. Acad. Sci. USA* **93,** 9339–9345.

O'Dowd, D. K., Gee, J. R., and Smith, M. A. (1995). Sodium current density correlates with expression of specific alternatively spliced sodium channel mRNAs in single neurons. *J. Neurosci.* **15,** 4005–4012.

Ruano, D., Lamoblez, B., Rossier, J., Paternain, A. V., and Lerma, J. (1995). Kainate receptor subunits expressed in single cultured hippocampal neurons: Molecular and functional variants by RNA editing. *Neuron* **14,** 1009–1017.

Sajjadi, F. G., and Pasquale, E. B. (1993). Five novel avian Eph-related tyrosine kinases are differentially expressed. *Oncogene* **8,** 1807–1813.

Saldivar, J. R., Krull, C. E., Krumlauf, R., Ariza-McNaughton, L., and Bronner-Fraser, M. (1996). Rhombomere of origin determines autonomous versus environmentally regulated expression of *Hoxa-3* in the avian embryo. *Development* **122,** 895–904.

Sambrook, J., Fritsch, E. F., and Maniatis, T. (1989). ''Molecular Cloning: A Laboratory Manual.'' Cold Spring Harbor Laboratory Press, Cold Spring Harbor, NY.

Sasaki, H., and Kuroiwa, A. (1990). The nucleotide sequence of the cDNA encoding a chicken deformed family homeobox gene, Chox-z. *Nucleic Acids Res.* **18,** 184.

Schneider-Maunoury, S., Topilko, P., Seitanidou, T., Levi, G., Cohen-Tannoudji, M., Pournin, S., Babinet, C., and Charnay, P. (1993). Disruption of Krox-20 results in alteration of rhombomeres 3 and 5 in the developing hindbrain. *Cell* **75,** 1199–1214.

Sham, M. H., Vesque, C., Nonchev, S., Marshall, H., Frain, M., Gupta, R. D., Whiting, J., Wilkinson, D., Charnay, P., and Krumlauf, R. (1993). The zinc finger gene *Krox-20* regulates *Hoxb-2* (*Hox2.8*) during hindbrain segmentation. *Cell* **72,** 183–196.

Smith, M. A., and O'Dowd, D. K. (1994). Cell-specific regulation of agrin RNA splicing in the chick ciliary ganglion. *Neuron* **12,** 795–804.

Sundin, O. H., Busse, H. G., Rogers, M. B., Gudas, L. J., and Eichele, G. (1990). Region-specific expression in early chick and mouse embryos of Ghox-lab and Hox 1.6, vertebrate homeobox-containing genes related to *Drosophila labial*. *Development* **108,** 47–58.

Sundin, O. H., and Eichele, G. (1990). A homeo domain protein reveals the metameric nature of the developing chick hindbrain. *Genes Dev.* **4,** 1267–1276.

Swiatek, P. J., and Gridley, T. (1993). Perinatal lethality and defects in hindbrain development in mice homozygous for a targeted mutation of the zinc finger gene Krox-20. *Genes Dev.* **7,** 2071–2084.

Vesque, C., Maconochle, M., Nonchev, S., Ariza-McNaughton, L., Charnay, P., and Krumlauf, R. (1996). Hoxb-2 transcriptional activation in rhombomere-3 and rhombomere-5 requires an evolutionarily conserved cis-acting element in addition to the Krox-20 binding-site. *EMBO J.* **15,** 5383–5396.

Wilkinson, D. G. (1992). ''*In Situ* Hybridization: A Practical Approach,'' pp. 75–83. IRL Press, Oxford/New York/Tokyo.

Wilkinson, D. G., Bhatt, S., Chavrier, P., Bravo, R., and Charnay, P. (1989a). Segment-specific expression of a zinc-finger gene in the developing nervous system of the mouse. *Nature* **337,** 461–464.

Wilkinson, D. G., Bhatt, S., Cook, M., Boncinelli, E., and Krumlauf, R. (1989b). Segmental expression of Hox-2 homeobox-containing genes in the developing mouse hindbrain. *Nature* **341,** 405–409.

Received for publication February 6, 1997
Accepted August 13, 1997